Phys. Status Solidi A **206**, No. 7, 1636–1640 (2009) / **DOI** 10.1002/pssa.200824469

physica status solidi a
www.pss-a.com
applications and materials science

Highly sensitive spin-valve devices for chip-cytometers

Jong Wook Roh[1], Oh-Taek Son[2], Young Tack Lee[1], Kyoung-il Lee[1], Hyo-Il Jung[,2], and Wooyoung Lee[*,1]**

[1] Department of Materials Science and Engineering, Yonsei University, 134 Shinchon, Seoul 120-749, Korea
[2] School of Mechanical Engineering, Yonsei University, Seoul 120-749, 134 Shinchon, Seoul 120-749, Korea

Received 13 November 2008, revised 28 January 2009, accepted 9 February 2009
Published online 23 April 2009

PACS 75.20.–g, 75.47.De, 87.80.–y, 87.85.dh, 87.85.fk

[*] Corresponding author: e-mail wooyoung@yonsei.ac.kr, Phone: +82 2 2123 2834, Fax: +82 2 312 5375
[**] e-mail uridle7@yonsei.ac.kr, Phone: +82 2 2123 5814, Fax: +82 2 312 2159

The highly sensitive spin-valve devices integrated with a microfluidic channel have been studied for cell counting in a chip-cytometer. The presence or absence of a single magnetic bead was successfully detected by direct measurement of fringe fields emanating from magnetic beads using spin-valve devices. The real-time detection was also successfully confirmed by the direct measurement of magnetic fields generated from the magnetic beads passing an active sensing area of a spin-valve device integrated with a microfluidic channel. Our results show the possibility of implementing a chip-cytometer for biological applications using the highly sensitive spin-valve devices integrated with a microfluidic device.

© 2009 WILEY-VCH Verlag GmbH & Co. KGaA, Weinheim

1 Introduction For the past several years, magnetic labels and their detection have been employed in biochip technology for genetic disease diagnostics, antigen–antibody interaction and cell separation [1–6]. In these experiments, magnetic beads were used to label target bimolecules that eventually hybridize with immobilized probes. To measure the quantity of labeled bimolecules, the magnetic beads were often tagged by fluorescent materials and the signal was analyzed by an expensive imaging system [7]. In order to overcome these limitations, there have been reported electrical-detection methods of magnetic beads using magnetoresistance (MR) sensors [8, 9]. Compared to fluorescent-material-based optical biodetection, the MR sensors-based magnetic-bead detection has the advantages of less complex instruments, faster analysis time, and lower cost. To date, the MR sensors-based magnetic-bead detection is rather limited to a molecular recognition assay rather than biological cell counting because the MR sensor detects beads immobilized tightly on the sensor surface in a molecular recognition assay, whereas the real-time detection of the flowing beads should be read by the sensor in order to separate and detect the target cells, simultaneously.

In our previous work, we have succeeded in separation of target cells (i.e. apoptotic cells) coated with magnetic beads from a cell mixture in a microfluidic channel with 96% accuracy, and an optical method was adopted to count the separated cells [10]. To increase the accuracy of experiments and decrease the labor required in the optical measurement process, we intend to introduce a chip-cytometer using MR sensors for the detection. Figure 1 presents the conceptual drawing of a chip-cytometer designed for detection of the flowing magnetic beads in a microfluidic channel. The chip-cytometer consists of integrated MR sensors and a microfluidic channel. The inlet of the microfluidic channel introduces normal cells and magnetic-beads-coated target cells in buffer solution. Magnetic-beads-coated target cells travel with normal cells together through the microfluidic channel. When the magnetic-beads-coated target cells pass over the MR sensors, the magnetic dipole field of the magnetic beads, generated by the external magnetic field from electromagnet, cancels a small fraction of the external magnetic field at the MR sensors, resulting in a change of sensor signal. From a technological point of view, one of the crucial issues in developing a chip-cytometer is to demonstrate the real-time detection of magnetic beads moving in a microfluidic channel using sensing elements, for which high sensitivity, good signal to noise ratio (S/N) and a low detection limit are required. Spin-valve devices have been reported to

WILEY InterScience® DISCOVER SOMETHING GREAT

© 2009 WILEY-VCH Verlag GmbH & Co. KGaA, Weinheim

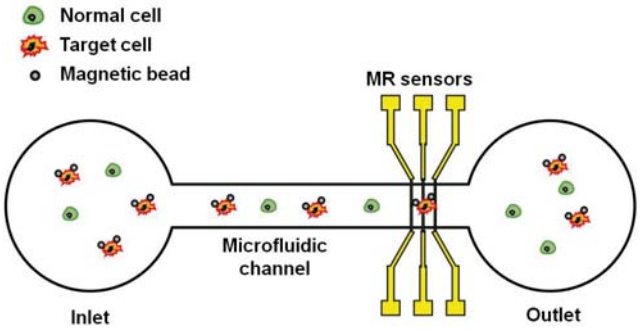

Figure 1 (online colour at: www.pss-a.com) A conceptual drawing of MR sensors integrated into a microfluidic channel. The magnetically labeled target cells are only counted using MR sensors.

meet such requirements sufficiently as sensing elements for a chip-cytometer [9, 11], which are more advantageous than other spintronic devices, such as giant magnetoresistance (GMR) devices [12], anisotropic magnetoresistance (AMR) devices [13], Hall effect devices [14] and magnetic tunneling junction (MTJ) devices [15]. For these reasons, spin-valve devices are expected to be a good candidate to detect moving magnetic beads in a microfluidic channel for cytometer applications.

In the present work, we report real-time detection of single micrometer-sized superparamagnetic beads using highly sensitive spin-valve devices integrated into a microfluidic channel for the application of the spin-activated cell counting in a chip-cytometer. We will describe labeling of target cells with magnetic beads first, and then will discuss the detection of magnetic beads using spin-valve devices with respect to the static and dynamic measurements.

2 Experiment Prior to detection of target cells in a chip-cytometer, it is required to verify that target cells are labeled with magnetic beads. In this experiment, apoptotic cells, which are the main type of programmed cell death, were utilized as the target cells [10]. In Fig. 2a, we illustrate a schematic diagram of labeling apoptotic cells with magnetic beads. Biotin-C2A protein, drug-treated Jurkat cells, and $CaCl_2$ were mixed and then incubated for 10 min. Then, streptavidin-coated magnetic beads were added and mixed gently for 20 min at room temperature. Phosphate buffered saline (PBS) was added up. Finally, apoptotic cells coated with magnetic beads were filtered using a centrifugal prefilter (NY41, Millipore), whose pore was 40 μm in diameter to eliminate the aggregates of beads and cells. Figure 2b and c show optical microscopic images showing apoptotic cells without labeling magnetic beads and magnetically labeled apoptotic cells, respectively. Protein C2A-biotin acts as a molecular linker between a cell membrane that has phosphatidylserine (PS) exposed on the outer surface and magnetic beads coated with streptavidin. Magnetic beads were found to be attached on the surface of apoptotic cells by comparing between before and after incubation with a combination of protein C2A-biotin and magnetic beads.

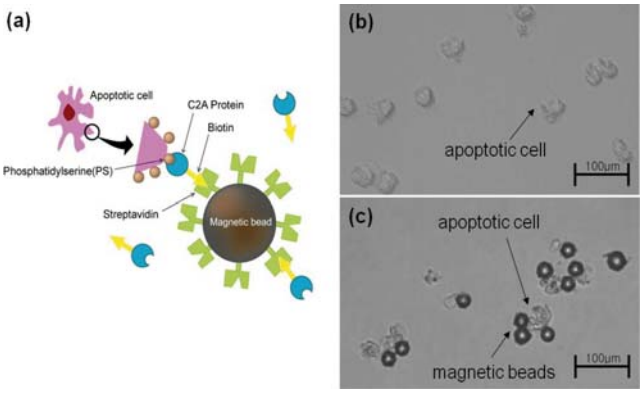

Figure 2 (online colour at: www.pss-a.com) Schematic diagram of selectively labeled apoptotic cells (a). Optical microscope images of the apoptotic cells before being conjugated with magnetic beads (b) and after the conjugation (c).

Spin-valves were deposited on a thermally oxidized Si(100) substrate in a dc/rf magnetron sputtering system with a base pressure of 4×10^{-8} Torr. The generic structure of the spin valves was $Co_{84}Fe_{16}$ (20 Å)/NOL/$Ni_{81}Fe_{19}$ (25 Å)/

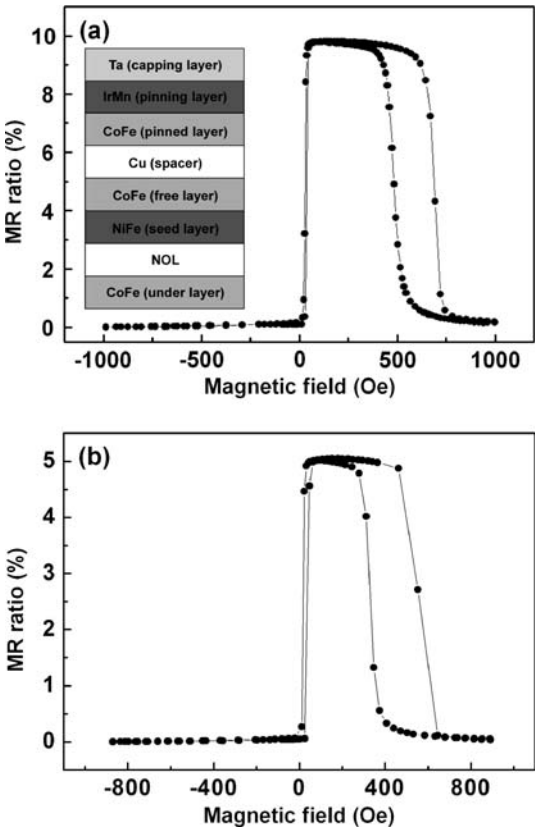

Figure 3 (a) Magnetoresistance (MR) curves of a spin-valve continuous film. The inset illustrates the generic structure of the spin valve. (b) MR curves of a spin-valve device fabricated from the continuous film. The best sensitivity in the MR of a spin-valve device was found to occur in the range 25–50 Oe.

© 2009 WILEY-VCH Verlag GmbH & Co. KGaA, Weinheim

$Co_{84}Fe_{16}$ (10 Å)/Cu (17 Å)/$Co_{84}Fe_{16}$ (20 Å)/$Ir_{22}Mn_{78}$ (75 Å)/Ta (50 Å). The nano-oxide layer (NOL) was employed in order to enhance the sensitivity of the spin valves [16]. As-deposited spin valves were found to exhibit about 10% magnetoresistance (MR) ratio as shown in Fig. 3a. Spin-valve devices with dimension of $6 \times 30\ \mu m^2$ were fabricated using a combination of photolithography and a lift-off process. The aspect ratio of 1:5 was selected in order to decrease the demagnetizing fields and to increase the sensitivity of the spin-valve devices. The patterned spin-valve devices were measured to be ~5% MR as shown in Fig. 3b, and were used for both static and dynamic measurements. The reduction of MR ratio is attributable to the lead contact resistance. In this work, all experiments were carried out with 1 μA of a sensing current. The surface of the spin-valve devices was passivated with a 200 nm thick silicon dioxide using a radio frequency (rf) sputtering system in order to prevent device corrosion due to the buffer solution.

In order to transport magnetic beads toward the active sensing areas of the spin-valve devices, a polydimethylsiloxane (PDMS) microfluidic channel was fabricated using soft-lithography. The epoxy-based negative photoresist SU-8 2025 (MicroChem) was applied to fabricate a microfluidic channel 30 μm high. After preparing the SU-8 mold, the template was placed in vacuum desiccators with Trichloro (1H,1H,2H,2H-perfluorooctyl) silane (Sigma Aldrich). We then poured the PDMS gel mixture (DC 184-A:B = 9:1, Dow Corning) on the SU-8 mold. Finally, the PDMS microfluidic channel was peeled off from the SU-8 master. In order to integrate a microfluidic channel and spin-valve devices, the direct-bonding method using O_2 plasma was utilized [17]. The O_2 plasma surface activation of both surfaces of a PDMS microfluidic channel and spin-valve devices was carried out for 30 s with rf plasma power of 100 W under O_2 pressure of 0.3 Torr. Then, two activated surfaces were allowed to come into contact at room temperature. As shown Fig. 4, the integration of the spin-valve devices into the microfluidic channel was successfully achieved using O_2 plasma direct bonding.

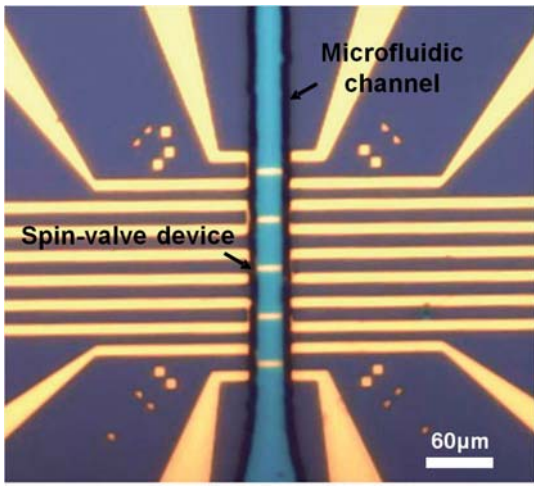

Figure 4 (online colour at: www.pss-a.com) An optical microscope image of the spin-valve devices array integrated with a microfluidic channel using O_2 plasma direct bonding.

3 Results and discussion Figure 5 displays a scanning electron microscope (SEM) image of a single magnetic bead with $d = 8.8$ μm (SPHERO™ SVM-80-5) located on the active sensing area of a spin-valve device. The SPHERO™ SVM-80-5 magnetic beads were streptavidin-coated superparamagnetic particles. The detection of a single magnetic bead in the static state has been investigated using patterned a spin-valve device, prior to the real-time detection of magnetic beads moving in a microfluidic channel. In order to place a single magnetic bead on the active area of a spin-valve device, we adopted a photolithography and lift-off process. A window in a photoresist layer, required to place a single magnetic bead on the active area of the spin-valve device, was patterned by photolithography. After dispersing the magnetic beads on the photoresist layer and removing the photoresist layer using a solvent, a single magnetic bead only was observed to be stuck to the surface of the spin-valve device due to van der Waals force between the surface of silicon dioxide layer and streptavidin of magnetic bead as shown in Fig. 5.

Figure 6 exhibits (a) MR curves of the spin-valve device with and without a single magnetic bead placed on the active area of the spin-valve device and (b) the resistance difference (ΔR) between the two MR curves. External fields (H_{ext}) were applied to the longitudinal direction of the spin-valve device in Fig. 5 using an electromagnet in order to induce a magnetic moment from the superparamagnetic bead and bias spin-valve devices, allowing these to operate in most sensitive areas. The MR curve was found to be shifted by 5 Oe, when the single magnetic bead was placed on the active area of the spin-valve device. The shift of the MR curve is ascribed to magnetic dipole fields emanating from the magnetic bead. It is clear that the shift was also confirmed by $\Delta R = R_{after} - R_{before}$, where the R_{before}

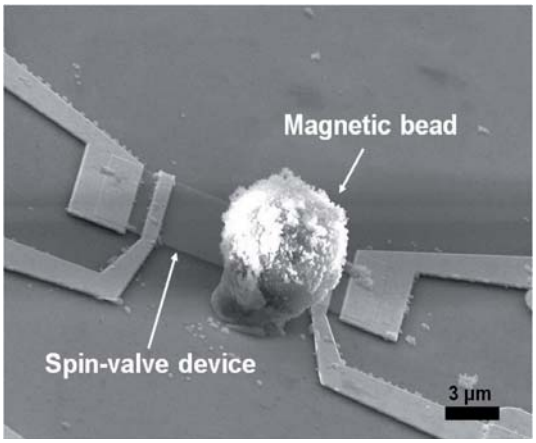

Figure 5 A SEM image showing a single magnetic bead on the active area of a spin-valve device.

© 2009 WILEY-VCH Verlag GmbH & Co. KGaA, Weinheim

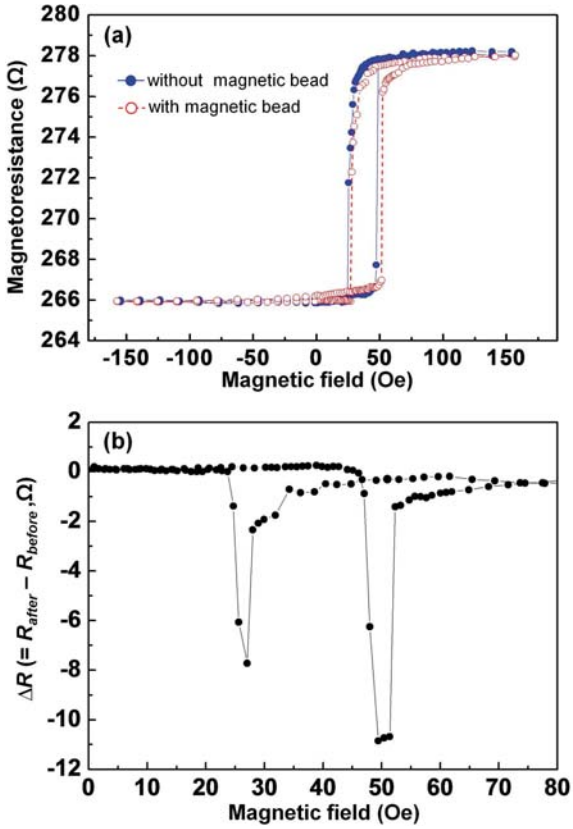

Figure 6 (online colour at: www.pss-a.com) (a) MR curves of the spin-valve device before and after placing a single magnetic bead, (b) resistance difference between the two MR curves.

and R_{after} are the resistances before and after placing the single magnetic bead, respectively as shown in Fig. 6b. When the magnetic bead was located on the active area of the spin-valve device, the magnetic dipole fields of the magnetic bead cancel out a small fraction of the applied fields in the free layer of the spin-valve device [18, 19]. The reduction of the applied field in the free layer gives rise to the shift of the MR curve. Our results demonstrate that our spin-valve devices are sensitive enough to detect a single magnetic bead.

Figure 7 shows an optical microscope image of an array of spin-valve devices integrated with a microfluidic channel, in which a supermagnetic bead flows. Superparamagnetic beads (Dynabeads® M-280) with $d = 2.8$ μm and a susceptibility of ~0.04 were utilized for the real-time detection. Dynabeads® M-280 are polymer beads with dispersion of iron oxide (γ-Fe_2O_3) nanoparticles. The magnetic beads dispersed in deionized water were funneled into the microfluidic channel using a syringe pump. The channel size used in our experimental had a height of 30 μm and a width of 30 μm. The length of channel is about 12 mm from center of inlet to center of outlet. The channel length was determined by computer simulations (incompressible Navier–Stokes module in COMSOL 3.2b. COMSOL Inc.) in order to optimize the motion and flow

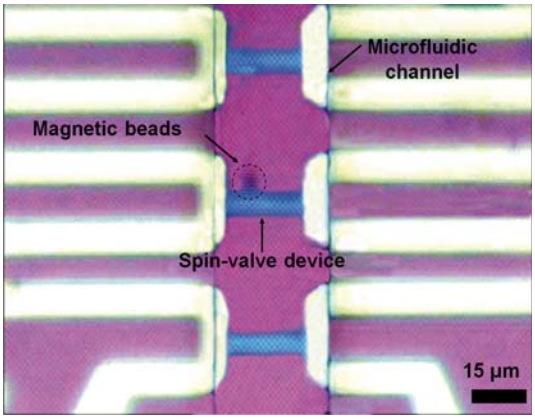

Figure 7 (online colour at: www.pss-a.com) An optical microscope image of the spin-valve devices and a magnetic bead moving in the microfluidic channel.

rate of magnetic beads in a microfluidic channel. It was found that the required channel length to flow before arriving at the bottom and the velocity of the particle after settling down at a flow rate of 0.01 l/min was 0.92 mm and 85 μm/s, respectively. In real-time detection, the fluid flow was controlled at a flow rate of 0.01 μl/min in order to roll the magnetic beads along the bottom surface of the microfluidic channel, as confirmed by the simulated results.

Figure 8 presents the real-time signals showing the detection of moving magnetic beads in the microfluidic channel. The most sensitive in the MR curve of a spin-valve device was found to occur in the range 25–50 Oe. A dc magnetic field (H_{ext}) of 30 Oe was applied to the longitudinal direction of the spin-valve devices in order to bias the free layer of the spin-valve devices and to generate a magnetic dipole field of the magnetic beads. Since H_{ext} was kept constant during the real-time detection, the signal voltage was only changed by the presence of a magnetic dipole field of magnetic beads. When a magnetic bead approaches the active sensing area of the spin-valve devices, a magnetic dipole field of the magnetic bead is expected to cancel out a small fraction of the applied field in the free layer of the spin-valve devices [18, 19]. The reduction of the applied field in the free layer was found to result in a signal voltage drop as seen Fig. 8. It is found that each signal voltage drop shows good agreement with an event that a single magnetic bead pass over the active sensing area of the spin-valve devices using an optical microscope and a charge-coupled device (CCD) camera integrated with measurement setup. The signal voltages of 0.33 μV and 0.41 μV were found to sharply drop at 125 s and 373 s, respectively. Such signal voltage drops are attributable to magnetic fields emanating from single magnetic beads passing over the active area of the spin-valve devices. The signal voltage was observed to recover the initial voltage as the magnetic beads completely passed over the active area. The signal recovery to the initial state shows that flow of buffer solution makes no change in signal voltage without magnetic beads.

© 2009 WILEY-VCH Verlag GmbH & Co. KGaA, Weinheim

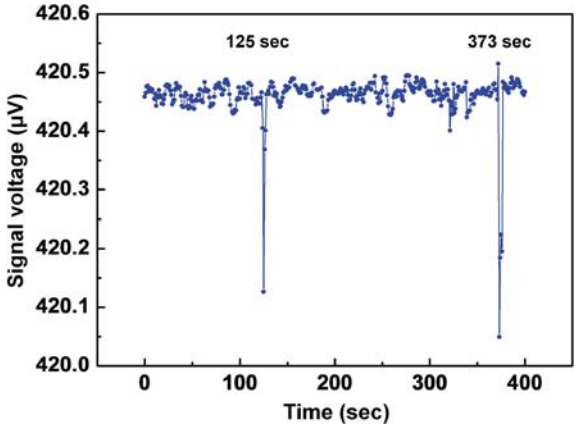

Figure 8 (online colour at: www.pss-a.com) Real-time signals showing the detection of moving magnetic beads in the microfluidic channel. Sharp signal drops were observed at 125 s and 373 s, respectively. The signal drops are attributed to a magnetic field emanating from respective magnetic beads passing over the active area of the spin-valve device.

The maximum magnetic dipole field (B^{max}) generated from magnetic beads (Dynabeads® M-280) was calculated using the equation of $B^{max} = -(\mu_0/4\pi)m_0/z^3$, where μ_0 and m_0 is a magnetic permeability and magnetic moment of magnetic beads, respectively [9]. The distance between the center of magnetic bead and the active sensing layer of spin-valve device (z) consists of the magnetic radius and thickness of passivation layer. B^{max} of Dynabeads® M-280 was estimated at 0.8 Oe, corresponding to signal voltage change of about 0.4 μV in the used devices. This value of calculated signal voltage change was consistent with the signal voltage change caused by a magnetic dipole field generated from magnetic beads in our dynamic measurements, demonstrating the real-time detection of single magnetic beads flowing in the microfluidic channel using the spin-valve device.

4 Conclusion The detection of magnetic beads using highly sensitive spin-valve devices integrated into a microfluidic channel for the application of the spin-activated chip-cytometer has been investigated with respect to the static and dynamic measurements. In the static measurement, a spin-valve device was found to show a shift of 5 Oe in the magnetoresistance curve in the presence of a single magnetic bead. Before carrying out the dynamic measurement of magnetic beads, the required channel length to flow before arriving at the bottom and the velocity of the particle after settling down at a flow rate of 0.01 l/min was investigated by computer simulation. According to the simulation results, the length of the microfluidic channel was determined in order to roll the magnetic beads along the bottom surface of the microfluidic channel. O_2 plasma surface activation was applied to bond the fabricated microfluidic channel and the spin-valve devices. In the dynamic measurements, the signal voltages of 0.33 μV and 0.41 μV were found to sharply drop at 125 s and 373 s, respectively due to magnetic fields emanating from the magnetic beads. Our results demonstrate the possibility of implementing a chip-cytometer for biological applications using the highly sensitive spin-valve devices integrated with a microfluidic device. Further studies will be extended to the fabrication of high-density spin-valve device arrays to improve the performance and the real-time detection of animal cells coated with magnetic beads for biological applications.

Acknowledgements This work was carried out via a grant from the program of KOSEF through the National Core Research Center for Nanomedical Technology (R15-2004-024-00000-0), the Seoul Research and Business Development Program (10816) and the Korea Research Foundation (MOEHRD, KRF-2005-042-D00203).

References

[1] M. M. Miller, P. E. Sheehan, R. L. Edelstein, C. R. Tamanaha, L. Zhong, S. Bounnak, L. J. Whitman, and R. J. Colton, J. Magn. Magn. Mater. **225**, 138 (2001).
[2] J. W. Choi, K. W. Oh, J. H. Thomas, W. R. Heineman, H. B. Halsall, J. H. Nevin, A. J. Helmicki, H. T. Henderson, and C. H. Ahn, Lab Chip **2**, 27 (2002).
[3] K. S. Kim and J. K. Park, Lab Chip **5**, 657 (2005).
[4] N. Pamme and C. Wilhelm, Lab Chip **6**, 974 (2006).
[5] C. D. Chin, V. Linder, and S. K. Sia, Lab Chip **7**, 41 (2007).
[6] R. Rong, J. Choi, and C. H. Ahn, J. Micromech. Microeng. **16**, 2783 (2006).
[7] Y. Weizmann, F. Patolsky, E. Katz, and I. Willner, ChemBioChem **5**, 943 (2004).
[8] R. L. Edelstein, C. R. Tamanaha, P. E. Sheehan, M. M. Miller, D. R. Baselt, L. J. Whitman, and R. J. Colton, Biosens. Bioelectron. **14**, 805 (2000).
[9] M. Johnson (ed.), Magnetoeletronics (Elsevier Academic Press, San Diego, 2004), chap. 7.
[10] H. S. Kim, O. T. Son, K. H. Kim, S. H. Kim, S. Maeng, and H. I. Jung, Biotechnol. Lett. **29**, 1659 (2007).
[11] D. L. Graham, H. A. Ferreira, P. P. Freitas, and J. M. S. Cabral, Biosens. Bioelectron. **18**, 483 (2003).
[12] R. L. Edelstein, C. R. Tamanaha, P. E. Sheehan, M. M. Miller, D. R. Baselt, L. J. Whitman, and R. J. Colton, Biosens. Bioelectron. **13**, 731 (1998).
[13] L. Ejsing, M. Hansen, A. Menon, H. Ferreira, D. Graham, and P. P. Freitas, Appl. Phys. Lett. **84**, 729 (2004).
[14] P. A. Besse, G. Boero, M. Demierre, V. Pott, and R. Popovic, Appl. Phys. Lett. **80**, 4199 (2002).
[15] W. Shen, X. Liu, D. Majumdar, and G. Xiao, Appl. Phys. Lett. **86**, 253901 (2005).
[16] E. Hirota, H. Sakakima, and K. Inomata, Giant Magneto-Resistance Devices (Springer-Verlag, Berlin, 2002), pp. 94–99.
[17] K. C. Tang, E. Liao, W. L. Ong, J. D. S. Wong, A. Agarwal, R. Nagarajan, and L. Yobas, J. Phys. **34**, 155 (2006).
[18] D. L. Graham, H. A. Ferreira, and P. P. Freitas, Trends Biotechnol. **22**, 455 (2004).
[19] H. A. Ferreira, D. L. Graham, P. P. Freitas, and J. M. S. Cabral, J. Appl. Phys. **93**, 7281 (2003).

© 2009 WILEY-VCH Verlag GmbH & Co. KGaA, Weinheim